High power laser components

Detlev Ristau* **and Henrik Ehlers**

Laser Zentrum Hannover e.V., Department of Thin Film Technology, 30419 Hannover, Germany

**E-mail: d.ristau@lzh.de*

Received October 31, 2009

Before going into the background of challenges imposed by modern laser technology on coated optical components, this letter reviews the major aspects of coating production and control. Current deposition techniques and characterisation methods for high power optical components applied in modern laser systems are summarised and discussed. In this context, methods are considered especially for the precise control of the spectral transfer properties of optical coatings during production. Also, a short review is presented regarding laser damage in optical coatings and the corresponding measurement techniques. In addition, the outlook includes recent developments in laser technology and corresponding trends in thin film production.

OCIS codes: 140.0140, 310.1860, 310.6860, 310.3840, 140.3330.

doi: 10.3788/COL201008S1.0140.

1. Introduction

Since the first demonstration of the laser principle at optical wavelengths in 1960, laser development has been one of the major pacemakers for the progress in production of optical laser components. Important steps in the fabrication of optical components involve the preparation of the bulk substrate material, the polishing of the optical surface, and finally, the deposition of a coating system governing the optical functioning of the component. In most applications, the optical coating system can be identified as the weakest link in the quality chain, which has to be optimized for the reliable performance of the component. As a consequence, the study of high power laser components is mainly concentrated on optical coatings and their precise characterisation. In the course of enormous improvements of laser output power and beam parameters, ever-increasing demands are imposed on optical coatings with respect to quality, stability, and precision. The present article is dedicated to these three major challenges and to recent progresses in the fields of optical coating, production, and quality control, as well as the optimization of the power handling capability of laser components. A brief review on modern trends in laser technology and on approaches in thin film technology to accomplish the corresponding prospective tasks is also presented.

2. Quality of Optical Coatings

The optical quality of coatings is mainly dependent on the intrinsic properties of the employed deposition material and the coating microstructure attained in the coating process. Since the spectrum of available deposition materials is naturally limited to only a few well-established and studied classes, the main optimization potential may be found in the deposition processes. However, an essential prerequisite for improvements in thin film quality is the measurement of the corresponding quality parameters with high precision and sensitivity. In the following section, before considering aspects of modern coating processes, a brief summary on the definition and measurement of the specific quality parameters for optical coatings is given.

2.1 Quality Parameters of Optical Coatings and Measurement Techniques

The characterisation of optical components, especially coating systems, has developed to an autonomous dynamic research area during the last two decades[1,2]. Besides the assessment of the dispersion properties of the constituent single layers, the determination of optical losses, stability factors, and defect densities of coating systems can be found in the foreground of present research activities. Optical losses, which can be divided into absorption and scattering, are of crucial importance for laser components, because they directly influence the technical performance and economic efficiency of a laser system or an application.

Absorption is defined by the amount of the incoming laser energy transferred into other energy channels such as phononic, electronic, or plasmonic excitations. In most cases, the generation of heat is the dominant effect of absorption and is often also the basis for corresponding measurement techniques. These methods probe and analyse quantitatively, for example, the temperature-induceed deformation of the coating surface, including thermal deflection[3,4] and thermal lensing[5], and an alteration of the environment near the surface (Mirage-effect)[6]. These techniques allow relatively fast measurements of absorption values down to the ms-regime, and surface mapping of absorption with spatial resolution in the μm-range. A technique based on the measurement of the laser-induced temperature rise in the components, allowing for a directly calibrated determination of absorption, is laser calorimetry. This concept was first implemented in the 1970s[7] and provided an uncomplicated access to calibrated absorption data via well-determinable measurement parameters, such as temperature rise, incoming laser power, and heat capacity of the sample. Since a direct temperature measurement in the sub-mK-range is essential for the measurement, laser calorimetry was previously believed to have insufficient sensitivity for modern laser components with absorption values of a few parts per million (ppm). However, recent studies indicate that the sensitivity of the

calorimetric method can be optimized to low values of approximately 0.02 ppm[8]. Also, international round-robin tests were conducted to evaluate the reproducibility and comparability of laser calorimetric data measured at different testing laboratories[9,10]. As a consequence, laser calorimetry has been established as a standard measurement technique (ISO 11551)[11] for absorption in optical laser components.

Scatter loss is defined by the amount of incident radiation deflected by the optical component out of the specular direction and into other solid angles. Fundamental measurement principles for scattered radiation are based on angle resolved scattering (ARS), which is a direct detection at each location around the sample, or on total scattering (TS), which is a collection of the radiation in the backward and forward half space of the sample. In most applications, TS is considered as a principal quality factor for scatter losses because the measurement of this parameter can be performed with a collecting Coblentz-sphere or an integrating Ulbricht-sphere with relatively low experimental effort. Also, for this type of measurements, a comprehensive measurement protocol (ISO 13696)[12] has been developed within international standardisation activities on the basis of comparative interlaboratory measurement campaigns[13]. Typical sensitivity values well below 1 ppm can be achieved for the visible spectral range with adapted TS-measurement facilities, thus, also allowing surface mapping of the specimen.

For laser applications with precisely confined wavelength ranges, the thermal stability of the coating may become a limiting factor. For example, in high-power diode-pumped solid-state lasers, the output beams of laser diode stacks are often combined by polarising beam splitters or wavelength filters to achieve high pump power levels of several kilowatts (kW) in the active laser material. As a result of the high power load, the combined elements are often operated under elevated temperatures and have to retain their complex spectral transfer characteristics over an extended temperature range. Therefore, the thermal stability of a laser component is often defined by the shift ($\delta\lambda$) of the spectral characteristic at a certain wavelength position (λ_0) induced by an increase of its temperature (ΔT). The corresponding shift value ($\delta\lambda/(\lambda_0\Delta T)$) can be measured with a spectrometer equipped with a temperature-controlled sample holder.

A variety of other quality parameters have to be considered for the assessment of laser components in different applications. Aside from the environmental, mechanical, and chemical impacts, laser-induced damage threshold (LIDT), the power handling capability of the component, also has to be considered. Since the LIDT is a limiting factor of utmost importance in many high power laser applications, it will be discussed in a separate section of this letter. In this context, the density of defects (defect density (cm^{-2})), which are often the initiation points of laser damage in the layer structure and on the surface of a laser component, also has to be taken into account as a principal quality parameter. The optical coating may also deform the surface figure of a component due to mechanical stress entailed by the coating on the substrate. The mechanical stress in the coating is determined by measuring the radius of curvature or bending of special substrates coated with the test layer and a subsequent evaluation on the basis of Stoney's formulae[14].

2.2 Deposition Processes for Laser Coatings

Presently, the predominant part of optical coatings for laser applications is deposited by physical vapour deposition (PVD) processes in vacuum. The fundamental production scheme of PVD processes comprise the release of the coating material in the form of a particle flux towards the substrates, the flight phase of the particles, and finally, the condensation of the particles on the growing layer structure. The different process types can be generally categorized according to the techniques employed for the production of the particle flux and to the conditions prepared for the condensation of the material. Thermal evaporation can be considered as the generic deposition technique involving a direct heating of the coating material and a condensation of the adatoms or admolecules under inert or reactive gas atmosphere. Depending on the materials and functional wavelength range of the desired coating systems, evaporation by a boat with resistive heating or by an electron beam is employed. Typical evaporation temperatures range between a few hundred and a few thousand degrees Celsius (°C) resulting in thermal energies of the adatoms characteristically below 0.3 eV. Therefore, the formation of the layer is governed by very limited mobility of the particles and shadowing effects. Particles impinging on the growing layer have only a confined effective reach and are often unable to occupy the optimum positions in the structure. Therefore, such coatings often exhibit a columnar microstructure (Fig. 1) with voids and a packing density lower than the value of the corresponding bulk material. Besides the reduced refractive index, which may be disadvantageous for coating systems with demanding spectral characteristics, the voids in the coatings may also adsorb matter from the environment, which may impede the performance of the system. Adsorbed water is a highly common occurrence and changes its concentration in the coating structure as a function of the environmental conditions. In turn, since water contributes to its refractive index of around 1.33 (visible spectral range) to the total optical thickness of the structure, the spectral characteristic of the layer is shifted with reduced water contents to lower wavelength. In particular, temperature has a dominant effect on the water contents in the layer inducing a substantial negative shift of approximately -100 ppm/°C. In addition, water adsorbed in the layer structure may be a factor for increased optical absorption in the coating, specifically in the range from 2.5 to 3 μm where OH-absorption bands are located. As an additional deficiency of thermal evaporated coatings, the surface topography of the layers is influenced by the fractal growth and reveals a relatively high roughness leading to significant optical scatter losses. In order to improve the quality of thermally deposited coatings, empirical investigations were performed regarding the dependence of the microstructural parameters on the material properties and deposition conditions. Prominent results of these studies are zone models that describe characteristic structural properties dependent on the ratio of the substrate temperature and the melting point of the coating material[15]. The zone models indicate a positive

effect of increased substrate temperature attributed to an augmented surface mobility of the particles condensing on a surface at higher temperatures. In practice, the deposition parameters are often optimized to achieve a maximum packing density and a balanced stoichiometry of the layers for each deposition material. Typically, for oxide materials, the elevated substrate temperature is around 300°C. To avoid stoichiometric deficiencies in the layers, reactive processes require an additional supply of oxygen. With optimized process parameters, relatively small absorption losses (below 10 ppm) and high LIDTs can be accomplished for mirrors in the near-infrared region with thermal evaporation. The major quality parameters of thermally deposited optical coatings are compiled in Table 1, in comparison to other advanced coating processes.

An analysis of the fundamental mechanisms in the condensation of the layer structure stipulates two major approaches to improving coating quality. On one hand, a significant increase in the surface mobility may support adatoms to occupy the optimum positions in the growing structure. For most materials, substrate heating alone cannot supply sufficient energy to attain high packing densities, and other techniques have to be introduced

Table 1. Quality Parameters for Different Process Concepts

Quality Parameter	e-beam	IAD	MS	IBS
Absorption (ppm)	< 10	< 10	$1-2$	< 1
Total Scattering (ppm)	< 100		< 10	< 1
LIDT (base e-beam)	1	0.5	0.1	0.25
T-Stability Typ. (ppm/°C)	-100	< 10	< 20	< 10
Coating Stress (100 MPa)	< 4	$(-)$ 1–2	$(-)$ 2–4	$(-)$ 8
Defect Density (cm^{-2})	< 100			< 1
Substrate Temper. (°C)	< 250	50–100	< 50	< 50
Rate (nm/s)	$1 - 10$	< 0.5	0.5	0.3–0.4
Coated Area (10^2 cm^2)	150	150	19	13
Productivity (10^2 nm·cm^2/s)	> 100	75	20	2

Estimation of characteristic quality factors of high-reflecting laser mirrors for the wavelength of the Nd:YAG-laser (1.064 μm) produced with conventional and ion processes (materials and deposition conditions selected for best effort). The notation for the damage threshold values (reference LIDT of best e-beam coating) is based on the results of the Boulder Damage Competition 2008 (Fig. 10[40]).

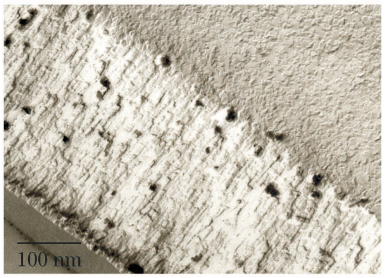

Fig. 1. Transmission electron micrograph of a MgF_2/LaF_3-coating system deposited by thermal evaporation. Total geometric thickness is 780 nm.

to improve the surface mobility of the adatoms. Corresponding approaches to deposit additional energy often include a generation of energetic ions, which are directed onto the growing layer. In these ion- or plasma-assisted deposition processes, the packing density is improved by a momentum transfer from the ions impinging onto the coatings, to the condensing adatoms. On the other hand, a clear improvement of the microstructural quality is expected if the layers are formed by adatoms bringing the necessary energy directly into the structure. Sputter processes, where the deposition material is released by sputtering from a target with energetic ions, are based on this principle. Subsequently, some aspects of advanced assisted and sputter deposition techniques for the production of high power laser coatings are considered.

Since the 1960s, several process concepts involving energetic ions for the layer structure compacting have been under investigation. Besides ion-plating processes, with the reactive low-voltage ion plating (RLVIP)[16], as the most prominent variant, ion-assisted deposition (IAD) has found its way into routine industrial production of high quality coatings. IAD processes are based on a separate ion source installed, in addition to the evaporation sources in the process chamber. The opening of the ion source is directed towards the substrates and delivers a flux of inert (noble gases) or reactive ions (oxygen, nitrogen, and fluorine) with energies in the range of a few tens up to hundreds of electron volts (eV), superimposed with the particles emitted by the evaporation sources. The dominant densification mechanism of momentum transfer[17] is additionally supported by a selection process, thus, removing only loosely bound atoms to the layer structure and conditioning the growing layer surface. As a consequence of these special growing conditions, an additional "zone T" with favourable properties appears in the structure zone model for IAD processes[18]. The adsorption of water in the layer structure and all the related negative effects on the coating quality can then be avoided. As such, the thermal shift of IAD coatings is no longer dominated by water desorption effects, but by the thermal expansion of the coating materials and the change of refractive index with temperature, leading to a significantly smaller positive shift of approximately 10 ppm/°C (Table 1). However, excessive ion energies may induce stoichiometric defects by the preferential sputtering effect, which results from different sputtering efficiencies of the single components of a compound[19]. In the case of metal oxides, which are widely used for high power coatings, preferential sputtering results in an

oxygen deficiency and, consequently, in an increase of the optical absorption losses[20]. Also, the optical absorption may be influenced by additional contamination introduced into the layer structure by material sputtered from the electrodes or grating system of the ion source. Often, the stoichiometric deficiencies induced by preferential sputtering can be compensated by reactive oxygen ions generated in the ion source with additional supply of oxygen into the discharge. Nevertheless, if extremely low absorption values of IAD coatings are intended, contributions of contamination effects and interface absorption deteriorate the coating performance. Therefore, the absorption of IAD-coated systems adjusts frequently to slightly higher values than achieved for corresponding conventional coatings. As a practical advantage, IAD processes permit the tuning of the mechanical intrinsic stress of a coating in a broad range, from tensile to compressive (Table 1). An optimization of the mechanical stress may be necessary to improve the layer adherence or to conserve the surface figure of the optical component, which may be deformed under the action of excessive stress. Furthermore, an implemented ion source can also be employed as a tool for conditioning of the substrates prior to or after the deposition of the coating.

The success of sputter processes in optical coating technology is based on the augmented energy of the adatoms forming the layer structure, and its potential for scaling to substrate dimension in the range of several meters. Therefore, sputter processes are predominantly employed for the coating of large automotive parts, foils, or architectural glass. For a considerable period, sputtering was considered as inappropriate for the deposition of high quality coatings because a relatively high base pressure had to be maintained to sustain an efficient discharge between the anode and the material target, which is necessary to generate the energetic ions for sputtering. However, during the last two decades, advanced plasma- and ion-assisted magnetron sputtering (MS) concepts have been cultivated also for applications in precision optics and laser technology. Significant progresses were achieved on the basis of dual magnetron (twin magnetron) configurations with medium frequency voltages in a typical range of 20 to 100 kHz. To prevent electrostatic charging as well as the disappearing anode effect, both target electrodes are alternately operated as cathode and anode. Furthermore, advances were accomplished in sequential processes with zones, where the material is deposited in metallic mode, and zones, where the metal is oxidized in a reactive or even activated reactive oxygen atmosphere. In addition, pulsed magnetron concepts have been developed to reduce thermal load on the target and the substrates. Today, modern MS systems can compete with other advanced deposition techniques with respect to absorption losses, stability, and reproducibility (Table 1).

A special class of sputtering process is ion beam sputtering (IBS), which was patented in 1978 by an aircraft company[21] in the course of the development of mirrors with the lowest back scattering necessary for laser gyroscopes. In this deposition concept, the energetic ions sputtering the target are produced by a separate ion beam source avoiding the contact of target or substrate with the discharge plasma necessary in conventional sputter techniques. Typical deposition conditions include ion energies in the range between 500 to 2000 eV and beam currents up to 1 A for efficient sputtering of the target material, which can also be a dielectric, if the ion source is operated in conjunction with a neutralizer. The energy of the sputtered adatoms can be adjusted in a range between a few and some tens eV, which is most advantageous for the formation of coatings with dense, amorphous microstructure (Fig. 2) as well as high optical quality. Also, the three major process steps in ion generation, sputtering, and condensation are well separated within the IBS process and can be performed under clearly defined environmental conditions. The residual gas atmosphere of the ion generation can be controlled independently, thus, allowing a reduction of contamination and a nearly ideal stoichiometry in the coatings. Finally, IBS processes offer an outstanding process stability and reproducibility, because they are defined only by a few process parameters, which can be well controlled. Therefore, IBS coatings are presently leading in many quality factors for laser components[22] and can be deposited with unsurpassed precision of the spectral characteristics. For example, mirrors with total optical losses below 1 ppm (Table 1) can be produced for the near infrared spectral range, and the precision is sufficient for the realization of very demanding coating systems used in femtosecond laser systems or optical inspection techniques.

All advanced deposition processes offer the advantage of low substrate temperatures, hence, allowing the processing of temperature sensitive substrates of polymers, frequency conversion, and laser crystals, or even electronic and mechatronic devices. Naturally, the de-

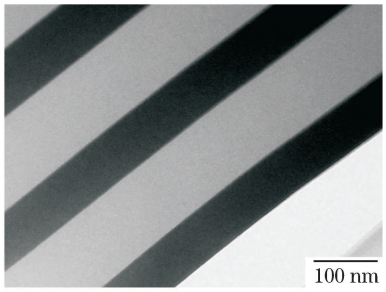

Fig. 2. Transmission electron micrograph of a single Titania layer (geometric thickness: 200 nm) deposited by IBS courtesy of J. Ebert, Laseroptik GmbH, Germany.

Table 2. Quality Parameters of Nb_2O_5-Layers

Quality Parameter	E-Beam	PIAD	IAD	MS	IBS
Refractive Index @500 nm	2.32	2.30−2.33	2.39−2.42	2.40	2.34
Extinction Coeff. @1064 nm ($\times 10^{-6}$)	45	15−40	13−15	6−14	3
T-Stability Typ. ($\times 10^{-5}$ ppm/°C)	−15	0.9	1.0	0.7	∼1

Quality parameters of Nb_2O_5 single layers (geometric thickness around 500 nm) deposited by different deposition processes (plasma ion-assisted deposition (PIAD)[25,26]).

position material also plays a key role in the quality ranking of deposition processes with respect to optical quality. For example, the production of optical coatings for lasers in the deep ultra-violet (DUV)/vacuum-ultraviolet (VUV)-range is mainly governed by fluoride materials deposited by conventional processes, which still achieve the best optical performance, even though intensive research is presently dedicated to an optimization of the ion processes[23,24]. The wavelengths of the CO_2-laser around 10.6 μm can be considered as a further region dominated by conventional processes, and typical non-oxide material combinations include ZnSe, ZnS, Ge, ThF_4, or YbF_3. For illustration of an exemplary optimization of oxide materials in the visible spectral range, the refractive indices, extinctions coefficients at a wavelength of 500 nm and temperature stability values are compiled in Table 2 for single layers of Niobium oxide (Nb_2O_5)[25,26]. Nb_2O_5 is considered an interesting candidate material for various laser applications with high economic efficiency and offers a relatively high optical quality for most deposition processes. With the exception of conventional processes, the extinction coefficient around 10^{-5} can be achieved for single layers with thermal shift values in the range of a few 10^{-5} ppm/°C.

Comparing the discussed deposition processes, economic aspects have also to been considered. The area deposition rate expressed in nm·cm^2/s can be regarded as a characteristic quantity for the productivity of the processes (last row in Table 1). In this context, the ion-assisted processes and sputtering are often limited by the output capabilities of the employed ion sources, leading to lower deposition rates than usual for conventional thermal processes. In IBS processes, the achievable beam current of the ion sources is the bottleneck to a further increase in deposition rates, leading to a relatively low productivity of this deposition concept. In contrast to this, conventional processes are distinguished by their outstanding productivity, which is based on high deposition rates from large-scale evaporation sources and corresponding large coating areas of more than 1 m^2 per batch. Therefore, conventional processes are still predominantly employed in the production of high-power laser components, and advanced processes are only subject to special components with demanding specifications. However, the vivid competition of the different production processes is consistently continued to attain the ever-improving quality parameters, especially the potential of the modern sputtering processes, is still not fully capitalized. New process concepts based on chemical vapour deposition (CVD)-techniques or "phase separation"[27] are under development to surpass the present quality level.

3. Precision of Optical Coatings

The rapid development of modern laser technology imposes ever-increasing demands on the production of high quality optical coating systems. For instance, innovative short pulse laser sources are dependent on optical coatings with a defined frequency chirp over a broad spectral range covering more than one octave. Frequency conversion systems and multi-wavelength applications call for high-quality coatings with defined characteristics, which are specified in small tolerance bands for several wavelengths and laser beam properties. In brief, a clear tendency towards optical coatings with more complex and broader spectral characteristics can be expected, and has to be mastered by future production concepts in optical thin film technology.

An approach towards this next generation of optical coatings may be based on production techniques geared to a linear production chain with a stable deposition process and a precise control system for the thickness of each single layer in the coating structure. Components for a successful implementation of this idea comprise of reliable tools to predict the result of a coating run, comprehensive process monitoring sensors and control algorithms, and strategies for the identification and correction of errors emerging during the deposition process. Obviously, the present optical coating production is still far away from this ideal situation, and additional efforts are necessary to approach this concept of deterministic production of optical thin films. Major aspects of deterministic optical coatings production are discussed elsewhere in detail[28], and therefore, only a brief review on the present state is presented in the following section before discussing the background of laser technology.

3.1 Virtual Deposition Processes

Coating designs for laser application gain an ever-increasing complexity, which leads to escalating risks in the production of coating systems. Thus, a consistent prediction of the results for a coating design in a production cycle is of enormous interest to avoid the costs for faulty deposition runs. Presently, software algorithms, which are able to emulate the coating process as a whole, are being studied by several research groups[29]. The development of such virtual deposition processes (VDP) precludes advanced coating processes with high stability and reproducibility. The major building blocks of the corresponding computer program include the simulation of the deposition process itself, the generation of virtual measurement data of the process monitoring devices, and the integration of the process-tracing algorithm for the determination of the actual state of the deposition, as well as for switching of the layers. Examples of the process monitoring devices include the single wavelength or broadband optical measurement systems, quartz crystal heads, oxygen sensors, and plasma probes.

In an implementation of a VDP concept in conjunction with an optical broadband spectrometer[30], the emulation of the layer deposition may consist of a routine (Fig. 3) that calculates the spectra of the produced layer structure in the actual state of deposition. Input data for the algorithm include all material data and significant coating parameters, as well as the time between the consecutive measurement cycles of the applied monitoring system. In the case of optical monitoring with direct measurement on the substrate, this measurement time would amount to the revolution time of the calotte. This period would also constitute the basic cycle time for the software algorithm defining the increments of the layer thickness in the simulation. The process is then simulated by consecutively generating spectra for thickness increments of the first layer until the switching point is reached. After material switching, the second layer is

built up in the same way to the switching point. This scheme is repeated for all subsequent layers until the design is completed. The algorithm also features an input mask for empirical deviations of the layer dispersion and for the emulation of typical technical errors occurring during the deposition run. In the present example, switching between the layers is controlled based on a simulation of a broadband monitoring (BBM) device that evaluates the calculated spectra, as shown in the right part of Fig. 3. The process tracing algorithm of the BBM calculates the thickness of the actual layer from the spectra on the basis of a least squares fit algorithm. In every cycle, this calculated thickness is compared to the target thickness of the simulated layer within the design. At a certain residual thickness left until switching, the layer termination routine is changed over to a time-counting mode with a termination time deduced from the deposition rates calculated in parallel. The switching points obtained in the simulation for each layer defines the simulated design as the result of the VDP analysis. This resultant design includes all deviations and errors, which are emulated by the VDP analysis based on empirical data with random simulation algorithms. This design differs from the projected coating design and will change from run to run of the VDP analysis. Considering the outcome of the VDP analysis, tendencies in the reproducibility of the design can be assessed, and layer systems with especially high risk of failure can be ruled out. Experiences obtained from the application of the VDP analysis for complicated design tasks indicate that two thirds of the designs pre-selected by the VDP algorithm lead to a successful production of the projected design in the first coating run.

3.2 Advanced On-line Monitoring

Presently, layer switching for demanding laser coatings is mainly performed based on single wavelength optical monitoring with flexible monochromator systems and sophisticated software packages, or with a spectrophotometric approach evaluating complete spectra of the growing layer system measured directly on the product. For sputtering processes with the highest stability, even time elapse modes are employed for switching. Very high precision in layer thickness have been demonstrated for single wavelength techniques, especially when self-compensation effects can be exploited for specific coating designs found in the production of complex filter systems for telecommunication or for laser technology[31]. However, for single wavelength monitoring, a separate strategy has to be developed and tested for each design. Optical broadband monitoring covers an entire spectrum measured directly from the growing layer system and employs the same control algorithm for all coating designs. In view of their flexibility, BBM concepts are considered as a resourceful basis for the implementation of deterministic production concepts and are presently in the focus of several studies on the reliable production of laser coatings.

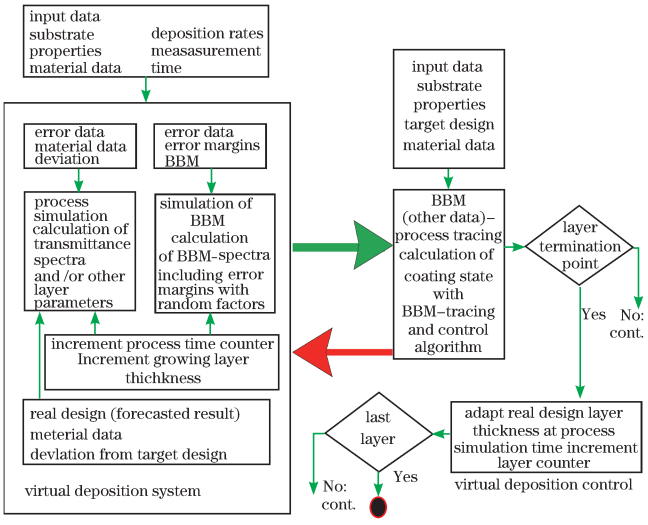

Fig. 3. Diagram of a VDP with a BBM system for deposition control. The fundamental structure consists of three units simulating the deposition process and the measurement channel of the on-line monitoring device. These two parts form the virtual deposition system. The virtual deposition control unit is illustrated at the right half of the diagram for a BBM system.

State-of-the-art BBM systems comprise a measurement routine synchronized to the substrate holder for a direct measurement of the growing coatings system on the actual product, as well as a self-calibration routine. Broad spectral ranges of more than one octave covering 300 to 1,100 nm can be attained by several spectrometers coupled with wavelength division multiplexing, or by spectrophotometers with specially adapted charge-coupled device (CCD) arrays. For specific designs, individual layer thickness accuracy values on the atomic scale can be attained with presently available monitoring systems. Improvements of spectrally resolved on-line monitoring might be achieved by the further extension of the spectral range, because more spectral features can be observed and evaluated within the layer switching routine. As a course rule, an increase in information available for the coating structure should result in a higher precision of the evaluations schemes and layer thickness control. In the same way, the accuracy of the measurement and the spectral resolution contribute to the reliability and sensitivity of the switching algorithm. New concepts for the simultaneous direct measurement of reflectance and transmittance could also increase the potential of optical monitoring. Particularly, losses and contaminations of the coating structures could be perceived during the coating process and employed for process optimization. Additional advantages are expected from a connection of optical monitoring systems to supplementary sensors in the deposition plant screening, for example, the deposition temperature, the composition of the gas atmosphere in the coating chamber, or the state of employed ion and evaporation sources. The coupling of a crystal monitor, which is used in most deposition plants for controlling the deposition rate, to an optical device suggests itself as a generic approach[28]. Such a combination compensates for the specific weaknesses of the two measurement methods. Optical monitoring suffers from a low sensitivity to layers with small thicknesses, because thin layers induce only a minute alteration in the spectral transfer function of the growing layer system. As a beneficial complement, the quartz crystal system delivers reliable measurement values for small thickness increments. Ac-

cordingly, a joint monitoring concept is expected to offer an extended thickness range of high switching precision.

3.3 Error Detection and Handling

Most deposition plants for sophisticated laser coatings are operated under continuous surveillance of personnel trained to recognize errors as they occur and to introduce corrections up to a certain degree of difficulty. However, the ideal deterministic production concept would function autonomously and must be combined with automatic error detection, as well as correction algorithms, to avoid deposition failures and the related economic losses. As an example, a combination of an optical monitoring system with a quartz crystal thickness measurement would open innovative perspectives to achieve such automatic error detection schemes. Apparent solutions can be formulated on the basis of a continuous recording and evaluation of the actual layer thickness based from quartz frequency data in parallel to the optical data. A substantial difference in the two thickness values may be considered as an indicator for an on-line error, and a suitable error management algorithm may be initialized. In the first approach, an error handling technique would include a permanent recalibration of the optical system by the crystal data, in order to overcome errors in optical thickness monitoring, which may occur due to erroneous dispersion of the layer or measurement uncertainties of the monitoring system. As an alternative approach, the crystal data may be employed for monitoring the thickness during most of the deposition time for each individual growing layer. When only a small fraction of the layer remains for deposition, the control algorithm may be switched to optical tracing to achieve the desired accuracy of the switching point[28].

The outlined strategies for deterministic coating production including a prediction of the result of a coating run and an accurate layer thickness control are dependent on the process stability. Advanced processes with a high reproducibility of the coating dispersion in an error margin around 1% seem to be appropriate for the implementation of present optical control systems. However, plasma- and ion-assisted techniques often suffer from higher variations in the refractive index, and are therefore dependent on more sophisticated control techniques, including error-handling routines that are also compensating for layer inhomogeneity effects. Currently, the specially integrated IAD processes developed in conjunction with a direct optical monitoring can achieve a very high accuracy and reproducibility[31].

4. Power Handling Capabilities of Laser Coatings

Output power is often an important factor for the versatility and the degree of acceptance of a laser concept in research and industrial applications. As a consequence, the development of laser systems operating at high power levels in a variety of wavelength regimes persists as a major task in global laser research. Currently, many laser concepts have advanced to the multi-kilowatt range in cw-operation, as well as at peak power densities on the petawatt level for pulsed systems. In the course of the corresponding research efforts, the power handling capability of optical laser components was often encountered as a major limiting factor. Similar to optical quality, the focus of research in laser-induced damage has shifted from the bulk to the surface, and especially to the coating of the optical component. Optical thin film technology has continuously accompanied laser development to achieve the demanding challenges with respect to power stability of the coatings[32]. The following section provides a brief glimpse of the field of laser damage in optical components, which has matured to a vivid research field in the last 40 years. In the first part, a summary is given on recent measurement techniques for the determination of LIDT values, which is also with regards to the International Standards. Furthermore, prominent damage mechanisms in optical materials and coatings are presented and discussed in the context of different pulse duration regimes of modern laser systems.

4.1 Measurement of LIDT

Reproducible and reliable measurement techniques for LIDT values are an indispensable prerequisite for a comprehensive optimization of laser components. The fundamental arrangement for an LIDT measurement facility comprises a laser system, an appropriate attenuator for adjusting the laser energy or power, and a focusing system that concentrates the laser energy onto the sample surface (Fig. 4). In early laser damage research, several protocols were employed for the testing sequence and the evaluation of the experimental data. Since the individual research groups relied on dissimilar test conditions, a comparison of results from different laboratories was relatively difficult and often was a source of misunderstanding within the research community. To cope with this problem, an extended international round-robin experiment was conducted on coated optics for the wavelength of 1.064 μm at the beginning of the 1980s[33]. A major outcome of this measurement campaign was the idea to standardize the measurement set-up and the underlying protocols for the determination of LIDT values. However, more than a decade of intensive discussion passed until a corresponding International Standard (ISO 11254[34]) was published. Aside from the measurement device, which is essentially similar to the previously described fundamental arrangement, the current Standard defines test sequences and adequate data reduction techniques for single (1-on-1) and multiple pulse (S-on-1) damage thresholds. The beam parameters of the laser are precisely monitored by a beam diagnostic system, which evaluates the spatial and temporal profile as well as the energy of the laser radiation in the target plane. The sample can be positioned with respect to the laser beam in distinct patterns, in order to investigate several sites with laser radiation, covering the entire inspection area of the sample. In a typical measurement sequence, each test site is objected to laser radiation with well-specified parameters and energy or power density value. In most cases, the laser is operated in single longitudinal and transversal mode to assure reproducible testing conditions.

In the test protocol according to the first part of ISO 11254 (1-on-1 testing), each test site is objected only once to a single laser pulse. A complete test sequence

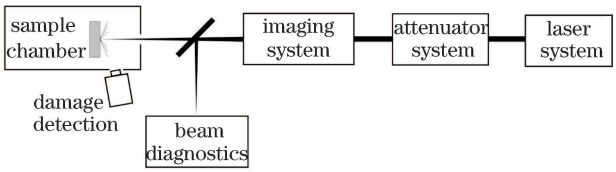

Fig. 4. Fundamental set-up for the measurement of LIDTs.

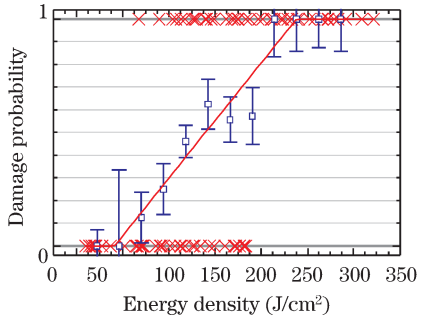

Fig. 5. Survival curve resulting from a single (1-on-1) damage test on a high-reflecting mirror of Ta_2O_5/SiO_2. As a test laser, a Nd:YAG system with a pulse duration of 14 ns and a beam diameter of 200 μm was employed. The results for the individual test sites are symbolized by crosses on the zero-bar (no damage) and unity-bar (damage occurred for the selected fluence). From this data, damage probability values (squares) were derived and plotted in the diagram. A linear fit to the probability value can be employed to determine the damage values from the intersection with the zero bar (onset value, 0%-LIDT) is 40.9±12.0 J/cm^2, while the probability 0.5 (50%-damage value, 50%-LIDT) is 139.0±12.0 J/cm^2.

consists of multiple interrogations with pulses of selected energies, covering a comprehensive range of fluence, with specific low values causing no damage, and high values consistently causing damage. For a reliable assessment of damage, the sample is inspected with a Nomarski interference contrast microscope, or other highly resolving surface measurement techniques, to identify the damaged sites after the irradiation procedure. Since each surface site is assigned to a certain laser energy or power, the elementary result of the damage test is a data row of fluence values in conjunction with the corresponding damage states. In ISO 11254−1, the final result of damage test is defined by a plot of the damage probability, which is calculated from the ratio of the number of damaged sites to the total number of sites objected to a certain fluence. This damage probability plot as a function of fluence is often called the survival curve of the optical component and provides an insight into the damage mechanisms involved. Finally, the damage threshold is given by the highest quantity of laser radiation for which the extrapolated probability of damage is zero. A typical example for a 1-on-1 damage test at the wavelength 1.064 μm and the extrapolated LIDT value is depicted in Fig. 5. Although 1-on-1 thresholds are predominantly of academic interest, they are often listed in many catalogues of optics manufacturers to illustrate the power handling capability of their products.

A test of more practical relevance involves a procedure with trains conveying a number of S identical pulses of defined laser fluence delivered to each site, which is described in the second part of ISO 11254 as S-on-1 test. In such test sequences, damage may occur before the full number of S pulses have been discharged on the sample site, resulting in a further expansion of the damaged area and, eventually, even in a catastrophic failure of the entire specimen. Hence, an online damage detection system is prescribed in the Standard, which should instantaneously interrupt the laser irradiation in the event of damage and should also include a pulse counter to record the number N of pulses until damage appears. In principle, the interrogation sequences and the subsequent sample inspection for the S-on-1 test are performed similar to the 1-on-1 test, revealing a data set with fluence values in conjunction with according numbers N until damage is observed or the total number S of pulses for sites without damage. Further data processing according to ISO 11254−2 yields the so-called characteristic damage curve of the specimen, which displays the energy density values for selected damage probabilities as a function of the number of pulses. An example for such a plot is depicted in Fig. 6 for samples measured with femtosecond laser sources. Besides a detailed fundamental interpretation in respect to damage mechanisms, characteristic damage curves offer also the advantage of a possible extrapolation to high pulse numbers in the order of 10^7 to 10^{10} shots. However, this approach to forecast the lifetime of optical components can be only considered as a very rough estimate and has to be confirmed by further individually adapted lifetime tests. An additional part of ISO 11254 had been published to characterize the certification of optical components with respect to their power handling capability. The described test protocols involve testing of a defined fraction of the sample surface at the laser energy level expected in the application. The fundamental approach of these tests is an assurance of a certain power level well above the upper limits of operation parameters encountered in practice.

The development of the International Standards had been assisted by several international round-robin tests, which were conducted to verify the reproducibility and practicability of the discussed measurement routines. Besides the ns-regime, the ultra-short pulse range was also addressed by international measurement campaigns. In Fig. 6, characteristic damage curves measured by several laboratories for a special mirror coating employed in the

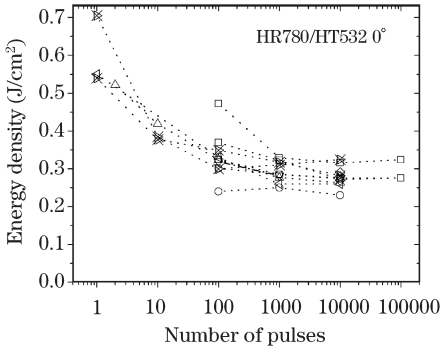

Fig. 6. Characteristic damage curves measured during a round-robin test on ISO 11254-2 for a laser mirror (HR 780 nm/HT 532 nm) coated on fused silica. The test conditions of the Ti:Sapphire lasers employed at the six participating laboratories varied in pulse duration between 130 and 150 fs and in beam diameter between 75 and 210 μm, respectively[35].

pumping scheme of Ti:Sapphire laser systems are plotted. Taking into account variations in the test parameters within this inter-laboratory test[35], the agreement of the characteristic damage curves is more than acceptable and reflects the versatility of the developed ISO Standard. Currently, a revised version of the Standard Series 11254 is under discussion by the corresponding standardization group. The major targets are the transfer of the experience gained in the application of the first standard series, the integration of more practical information, and a restructuring with respect to an improved practicability. The new series, which is assigned as Project Number 21254, also cover bulk damage of optical components and contain an additional technical report dedicated to damage detection, as well as sample inspection techniques.

4.2 Damage Mechanisms in Optical Coatings

Mechanisms governing laser-induced damage in optical coatings can be divided into effects, which are thermally induced by transformation of the impinging laser energy into heat, and processes driven by an intensive electronic interaction with laser radiation. In practice, damage processes on the basis of a direct absorption in the bulk of the layer structure are observed in optical coatings for lasers operated at the extreme spectral regions in the DUV/VUV-spectral range or in the mid-infrared. As a consequence of the strong absorption in these coatings, excessive heat is generated directly in the layer structure leading to elevated temperature levels that cause the thermal stress to exceed the adhesion strength, and hence, a delamination of the layers. At higher temperatures, the crystalline structure of the coating material may be altered and induce extremely high scatter losses. If the laser-induced temperature increases beyond the melting point of the materials, even an evaporation of the coating can be observed (Fig. 7). Enormous progresses in coating processes have led to an essential reduction of absorption in the visible and near-infrared spectral range below critical values of absorptive laser-induced damage. However, thermally induced effects initiated by absorbing defects in such layers still play an essential role in their power handling capability. Embedded defects with significantly higher absorption than the surrounding layer material absorb the impinging laser energy and heat up to extremely high temperatures until they explode in the layer structure, leading to craters in the layer system (Fig. 8). Ion sources, mechanical debris, discharges, or excessive deposits on the chamber wall may be identified as sources of defects introduced into the coating during the process. In addition, agglomeration effects or direct imperfections in the condensation process of the layer may lead to intrinsic defects with high absorption cross section. Recent studies dedicated to the controlled preparation of artificial defects in the layer structures demonstrate that even defects with sizes in the range of 10 nm may contribute to laser damage[36].

Direct electronic excitation effects derived from breakdown models for dielectrics under the action of strong electric fields have been discussed since the beginning of laser damage research. Most of the theoretical treatises assume that an excitation of electronic states by Avalanche- and Multiphoton-models builds up the electron density in the conduction band to a critical value,

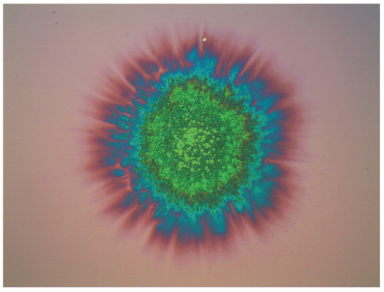

Fig. 7. Nomarski micrograph of a damage site on a single layer of Ta_2O_5 deposited by conventional evaporation (scale: horizontal image length ≈ 500 μm), which was occurred after one pulse (Nd:YAG-laser, wavelength 1.064 μm, beam diameter 200 μm, pulse duration 14 ns) at a fluence of 29 J/cm^2.

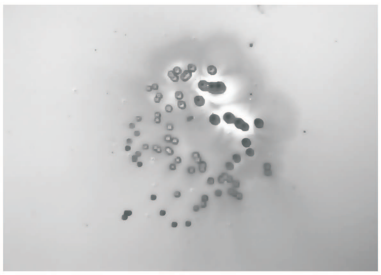

Fig. 8. Nomarski micrograph of a damage site on a coated sample (initiated at an energy density of approximately 17 J/cm^2 after 938 pulses of Nd:YAG-laser (S-on-1-test)) (scale: horizontal image length ≈ 500 μm).

where an irreversible damage of the material structure is induced by resonance absorption of the laser field. However, experimental evidence of these mechanisms, for example, scaling effects of the damage threshold with pulse width, wavelength, or beam diameter, could not be demonstrated until ultra-short pulse lasers found their way into high-power applications. For lower pulse durations in the ps- and fs-regime, thermal diffusion effects are too slow to contribute significantly to laser damage. Instead, below pulse durations of approximately $\tau = 20$ ps mainly electronic interactions on time scales in the fs- and as-range have to be considered for a theoretical conception of laser-induced damage. For a generic approach to damage mechanisms in the ultra-short pulse region, the electron density $\rho(t)$ in the conduction band of the dielectric material can be calculated based on a rate equation[37]

$$\frac{\partial \rho\,(t)}{\partial t} = W_{\mathrm{Pi}}(I(t)) + W_{\mathrm{Av}}(I(t), \rho(t)) - W_{\mathrm{rel}}(\rho, t). \quad (1)$$

In this model, two mechanisms are assumed for an excitation of electrons into the conduction band of the laser-irradiated material. One population effect may be attributed to the extremely high field strength of ultra-short pulse radiation. On the one hand, this may lead to a deformation of the electronic potential allowing for a direct tunneling of electrons into the conduction band. On the other hand, the probability of multiphoton effects increases with laser field strength, hence, additionally supports the generation of electrons in the conduction band. The corresponding term for the photon ionization rate W_{Pi} in the rate equation may be calculated

based on the Keldysh theory[38], which covers the tunneling, as well as the multiphoton effect, and contains a variety of material parameters. Avalanche ionization represents the second major excitation mechanism contributing to the rate equation. The corresponding term W_{Av}, which is dependent on the intensity $I(t)$ of the incident laser radiation and the electron density $\rho(t)$, represents the generation of free carriers by relaxation of a highly excited electron in the conduction band with energy transfer to a valence band electron to perform a transition to the conduction band. The third expression W_{rel} of the rate equation has been introduced to consider relaxation processes of free carriers from the conduction band to other electronic states induced by interactions with the lattice, structural defects, or color centers. For damage onset, a critical electron density of 10^{21} cm^{-3} near a plasma state in the conduction band is often assumed, leading to an instantaneous coupling of energy from the laser radiation into the plasma and to catastrophic damage of the material.

Generally, rate equations for distinct experimental conditions can be only solved numerically with approximations for the various necessary material parameters. Nevertheless, empirical studies can be performed to confirm some of the tendencies predicted by the model. One of the most significant projections of the model is the fundamental dependence of LIDT values on the band gap energies of the involved materials. The model also exclusively contains material constants and well-defined radiation parameters supporting the expectation that a deterministic behavior with a sharply defined onset of damage at a certain laser field strength should be observed in the ultra-short pulse regime. These tendencies could be demonstrated for coatings of sufficiently high optical quality[37], which can be achieved with ion beam sputtering processes. In the corresponding study, the LIDT values of IBS coatings of prominent oxide materials with various bad gap energies were measured with an ultra-short pulse laser system at pulse durations ranging from 15 fs to approximately 1 ps. A defined increase in threshold values with pulse duration and band gap energy E_{B} was observed, hence, demonstrating the relations expected from the theoretical model. The independence of the observed trends of the concrete material involved was an interesting aspect examined further by an experiment involving mixtures of the two oxide materials TiO_2 ($E_{\mathrm{B}} \approx 3.5$ eV) and SiO_2 ($E_{\mathrm{B}} \approx 5.4$ eV) with highest difference in band gap energies[39]. Coatings of these ternary oxides (ideally: $Ti_xSi_{1-x}O_2$) were produced with a reactive IBS process, based on a zone target with separate sections of Ti and Si. In this approach, the mixture ratio of the materials can be adjusted by the area of the two zones interrogating with the ion beam, and hence, by the position of the zone target with respect to the ion source. Ternary compounds with different mixture ratios specified by the parameter x were prepared and analyzed with respect to the power handling capability for ultra-short pulses in relation to the band gap energy. The results (Fig. 9) of this investigation evidently supported the outlined hypothesis and demonstrated furthermore, that the band gap energy of the mixture can be tuned by the mixture ratio. These interesting experimental findings are of major importance for the further optimization of optical coating systems for high-power femtosecond laser applications.

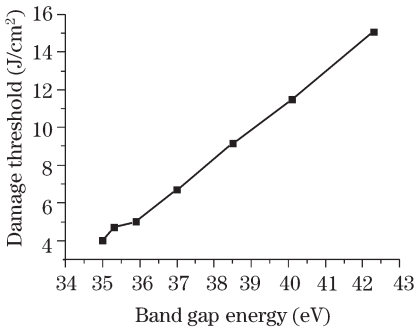

Fig. 9. LIDT values of ternary oxide ($Ti_xSi_{1-x}O_2$) coatings produced with an IBS process on the basis of a zone target. The damage thresholds (Ti:Sapphire laser, wavelength 780 nm, beam diameter 200 μm, pulse duration 230 fs) are plotted as a function of the band gap energy, which is directly related to the mixture ratio[39].

4.3 State of the Art in the Optimization of High Power Coatings

During the last four decades, extensive research work had been dedicated to the optimization of damage thresholds of optical components for all relevant laser wavelengths, among many others starting at 157 nm with the F_2-excimer-laser in the VUV-range, covering the harmonics of the Nd:YAG-laser, and ending at the prominent wavelength 10.6 μm of the CO_2-laser. To illustrate the present state of the art, selected results of an international damage competition arranged within in the framework of the 40th Boulder Damage Symposium in 2008[40] are depicted in Fig. 10. In this campaign, the damage thresholds of more than thirty HR-mirror samples delivered by industrial companies and research institutes from five countries were compared. At least six different deposition processes and material combinations of predominantly Ta_2O_5 and HfO_2 combined with SiO_2 were involved in the test. Best results of more than 120 J/cm^2 (Nd:YAG-laser operated at 1,064 nm, pulse length: 5 ns, 1/e^2-beam diameter: 1 mm^2) were achieved with e-beam deposition processes and HfO_2 as high index material. However, IAD processes and IBS were also found among the top 10% of the high-power coatings, indicating a high potential of these deposition techniques. Coatings with the material Ta_2O_5 were commonly observed to be more vulnerable to laser damage and reached only LIDT values of approximately one-third of the HfO_2-coatings. Analyzing the number of layers and interpreting an even number as indicator for the presence of an additional protection layer on the coating system showed evidence for a minor improvement of HfO_2-coatings by addition of an overcoat with the low index material. In contrast, no clear effects of overcoats were observed for the mirrors with Ta_2O_5 as high index material. However, these interpretations have to be considered within the context that some of the vendors declined from specifying their coating processes or deposition materials.

For a comprehensive optimization of the power handling capability, the complete production chain of the coating system has to be considered. As demonstrated

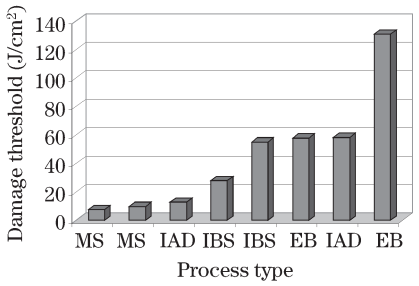

Fig. 10. LIDT values of high-reflecting mirrors for the Nd:YAG-laser (test conditions: 1.064-μm wavelength, 5-ns pulse length, 1 mm^2 1/e^2-beam diameter) selected (best and second best for each process type, the MS, IAD, IBS, and electron beam deposition (EB)) from the results of the Boulder Damage competition 2008[40].

for the wavelength of 1064 nm, the identification of the materials and their careful cultivation within the deposition process can be considered as key factors. In most of the cases, single layers can be optimized prior to coating systems, precluding that the damage behavior of the corresponding layer structures will be governed by the effects already observed for the constituent single layers. Once the optimum material combination has been found, the design of the coating structure shifts into the focus of the optimization strategy. The field strength distribution within the layer structure is of utmost concern and has to be adjusted in a way that the interfaces and materials that are more vulnerable to damage are subjected to lower field strength values than the more damage-resistant coating sections. Barrier layers to improve the adhesion or overcoats, to stabilize the outer layers of the coating system, are often employed to advance the damage resistance. In many cases, the power handling capability of the coating system suffers from laser induced effects located at the interfaces between the layers, where different material parameters and a reduced adhesion may contribute as detrimental factors. Therefore, present approaches to improved LIDT values involve the application of mixed materials and rugate filters to suppress interface effects. For instance, investigations in LIDTs of rugate filters of the material combination TiO_2/SiO_2 for ultra-short pulse lasers reveal a significant increase of the threshold values by nearly a factor of two[41] and even one order of magnitude for the ns-regime[42] in the near-infrared spectral range.

5. Summary and Outlook

During more than 40 years of intensive research, progresses in laser development and optical thin film technology have always been strongly interconnected. Modern laser applications impose ever-increasing challenges on the production of optical coating with respect to quality, precision, and power handling capability. In the field of deposition processes and the related optical quality, enormous advancements have been achieved with ion-assisted processes and innovative sputtering concepts. To control these stable processes, monitoring strategies involving several sensors have the potential to be precise, down to the atomic-scale layer thickness. Theoretical modeling and experimental studies on laser-induced breakdown phenomena remain a central point in the optimization of the power handling capability of optical components. In the present understanding of laser damage effects, thermal breakdown initialized by defects and absorption in the coating plays an important role for operation conditions ranging from continuous wave (CW)- to the ns-pulse regime. Damage in the ultra-short pulse region has been demonstrated to be mainly driven by the direct electronic interaction of the material with intensive laser radiation involving tunneling, multi-photon, and avalanche mechanisms.

Laser technology and its applications in the future will also remain important pacemakers for progresses in the field and directly define the upcoming tasks in optical thin film technology. Aside from the spectacular experiments in laser fusion, space born systems, and fundamental physics, industrial applications of lasers in material processing, medicine, information technology, and semiconductor lithography are considered as the most challenging domains with the highest economic potential. Ultra-short pulse lasers continue to gain interest in many applications, and there is a call for a new generation of high-power optics with improved spectral performance, including specification of reflectance and phase shift over a broad spectral range. Parallel to the ever-improving quality and precision, optical components have to meet new specifications such as extended lifespan and special environmental conditions. Semiconductor lithography follows its path towards half-pitch values of 30 nm in production with stepper systems employing water immersion. For these operation conditions at the wavelength of 193 nm, extended lifespan of the coatings for the stepper objectives have to be accomplished. Similar problems will be encountered in the next generation lithography, where optics for even smaller wavelengths (around 13 nm) have to be optimized to reach nodes ranging below 20 nm. The employed reflective optics have to withstand long-term high fluences at elevated operation temperatures of several 100 °C without changes in surface figure or optical quality. Furthermore, in the course of an increasing number of applications for lasers in space-born missions, the lifespan qualifications of optical components under vacuum conditions gain importance. Many laser applications call for a combination of optical quality and power resistivity with additional properties of the coatings. For instance, high-power laser coatings with improved mechanical or chemical stability for applications in laser medicine or components employed under severe industrial environment conditions have to be mentioned.

The authors thank the German Ministry for Education and Science (BMBF) for the financial support within the framework of the research project “Plasma Assisted Sputtering Processes” and within the research cooperation PluTO 13N10460, and Dr. Krüger, VDI-TZ Düsseldorf for promoting this project. Funding from the German Research Foundation (DFG) within the Cluster of Excellence 201, “Centre of Quantum Engineering and Space Time Research”, QUEST, is also gratefully acknowledged.

References

1. D. Ristau, Proc. SPIE **4099,** 91 (2000).
2. D. Ristau, Optics and Precision Engineering (in Chinese) **13,** 435 (2005).
3. M. A. Olmstead, N. M. Amer, S. Kohn, D. Fournier, and A. C. Boccara, Appl. Phys. A **32,** 141 (1983).
4. E. Welsch and D. Ristau, Appl. Opt. **34,** 7239 (1995).
5. B. Li, S. Martin, and E. Welsch, Opt. Lett. **24,** 1398 (1999).
6. A. C. Boccora, D. Fournier, and J. Badoz. Appl. Phys. Lett. **36,** 130 (1980).
7. D. A. Pinnow and T. C. Rich, Appl. Opt. **12,** 984 (1973).
8. K. Starke, I. Balasa, H. Blaschke, L. Jensen, M. Jupé and D. Ristau, in *Proceedings of Opt. Interfer. Coatings (OSA Technical Digest)* ThA1 (2007).
9. D. Ristau, H. Niederwald, D. Erdelyi, P. Meja, A. Giesen, W. Plaß, R. Krupka, M. Kennedy, E. Oertel, Z. Lu, T. V. Lee, K. M. Lee, H. E. Reedy, D. Scatena, N. Ellis, and D. Greening, Proc. SPIE **2714,** 120 (1996).
10. D. Ristau, U. Willamowski, and H. Welling, Proc. SPIE **3578,** 657 (1999).
11. ISO 11551: Optics and optical instruments. Lasers and laser related equipment. Test method for absorptance of optical laser components. International Standard. International Organisation for Standardisation, Geneva, 2003
12. ISO 13696: Optics and optical instruments. Lasers and laser related equipment. Test Method for Radiation Scattered by Optical Components. International Organisation for Standardisation, Geneva, 2002.
13. P. Kadkhoda, A. Müller, D. Ristau, A. Duparré, S. Gliech, H. Lauth, U. N. Reng, M. R. Schuhmann, C. Amra, C. Deumie, C. Jolie, H. Kessler, T. Lindström, C. G. Ribbing, and J. M. Bennett, Appl. Opt. **39,** 3321 (2000).
14. G. Stoney, Proc. Roy. Soc. Lond. **A82,** 172 (1909).
15. B. A. Movchan and A. V. Demchishin, Phys. Met. Metalloved. **28,** 83 (1969).
16. H .K. Pulker, W. Haag, M. Buhler, and E. Moll, in *Proceedings of 5th Int. Conf. on Ion and Plasma Assisted Techniques* (*Munich*) 299 (1985).
17. J. D. Targove and H. A. MacLeod, Appl. Opt. **27,** 3779 (1988).
18. J. A. Thornton, J. Vac. Sci. Technol. **11,** 666 (1974).
19. S. Berg and I. V. Katardjiev, J. Vac. Sci. Technol. **A17,** 1916 (1999).
20. J. B. Malherbe, S. Hofmann, and J. M. Sanz, Appl. Surf. Sci. **27,** 355 (1986).
21. D. T. Wei and A. W. Louderback, "Method for fabricating multi-layer optical films" U. S. Patent 4142958 (1978).
22. D. Ristau and T. Groß, Proc. SPIE **5963,** 315 (2005).
23. F. Sarto, E. Nichelatti, D. Flori, M. Vadrucci, A. Santoni, S. Pietrantoni, S. Günster, D. Ristau, A. Gatto, M. Trovó, M. Danailov, and B. Diviacco, Thin Solid Films **515,** 3858 (2006).
24. M. Bischoff, M. Sode, D. Gäbler, H. Bernitzki, C. Zaczek, and N. Kaiser, Proc. SPIE **7101,** 71010L (2008).
25. N. Beermann, H. Ehlers, and D. Ristau, in *Proceedings of Opt. Interfer. Coatings (OSA Technical Digest)* TuF6 (2004).
26. L. Jensen, M. Jupé, H. Mädebach, H. Ehlers, K. Starke, D. Ristau, W. Riede, P. Allenspacher, and H. Schroeder, Proc. SPIE **6403,** 64030U0 (2006).
27. QUEST, Quantum Engineering and Space Time Research, German Cluster of Excellence at the Leibniz University of Hannover, 2008.
28. D. Ristau, M. Lappschies, S. Schlichting, and H. Ehlers, Proc. SPIE **7101,** 71010C (2008).
29. D. Ristau, in *Proceedings of 10th OptiLayer-Workshop on Advanced Topics in Optical Thin Films (Hannover)* 27 (2006).
30. D. Ristau, T. Groß, M. Lappschies, and H. Ehlers, Appl. Opt. **45,** 1495 (2006).
31. A. Zoeller, M. Boos, H. Hagedorn, W. Klug, and C. Schmitt, in *Proceedings of Opt. Interfer. Coatings on CD-ROM (OSA, Washington, DC)* TuE10 (2004).
32. M. Hercher, J. Opt. Soc. Am. **54,** 563 (1964).
33. K. H. Guenther, T. W. Humpherys, J. Balmer, J. R. Bettis, E. Casparis, J. Ebert, M. Eichner, A. H. Guenther, E. Kiesel, R. Kuehnel, D. Milam, W. Ryseck, S. C. Seitel, A. F. Stewart, H. Weber, H. P. Weber, G. R. Wirtenson, and R. M. Wood, Appl. Opt. **23,** 3743 (1984).
34. ISO 11254: Optics and optical instruments. Lasers and laser related equipment. Test methods for laser induced damage threshold of optical surfaces. Part 1: 1 on 1-test, 2000, Part 2: S on 1 test, 2001, Part 3: Assurance of laser power handling capabilities, 2006, International Organization of Standardisation.
35. K. Starke, D. Ristau, S. Martin, A. Hertwig, J. Krüger, P. Allenspacher, W. Riede, S. Meister, C. Theiss, A. Sabbah, W. Rudolph, V. Raab, F. Grigonis, T. Rakickas, and V. Sirutkaitis, Proc. SPIE **5273,** 281 (2004).
36. S. Papernov and A. W. Schmid, Proc. SPIE **6403,** 64030D (2006).
37. J. Jasapara, A. V. V. Nampoothiri, W. Rudolph, D. Ristau, and K. Starke, Phys. Rev. B **63,** 045117/15 (2001).
38. L. V. Keldysh, Soviet Physics – JETP **20,** 1307 (1965).
39. D. Nguyen, I. Cravetchi, W. Rudolph, M. Jupé, M. Lappschies, K. Starke, and D. Ristau, Proc. SPIE **6720,** 67200C (2007).
40. C. J. Stolz, M. D. Thomas, and A. J. Griffin, Proc. SPIE **7132,** 71320C (2008).
41. M. Jupé, M. Lappschies, L. Jensen, K. Starke, and D. Ristau, Proc. SPIE **6403,** 1A1 (2006).
42. M. Jupé, M. Lappschies, L. Jensen, K. Starke, and D. Ristau, Proc. SPIE **6403,** 11-1 (2007).